Available online at www.sciencedirect.com
ScienceDirect
Trans. Nonferrous Met. Soc. China 24(2014) 907−914
Transactions of Nonferrous Metals Society of China
www.tnmsc.cn

Effects of Y on hot tearing susceptibility of Mg−Zn−Y−Zr alloys

Zheng LIU, Si-bo ZHANG, Ping-li MAO, Feng WANG

School of Materials Science and Engineering, Shenyang University of Technology, Shenyang 110870, China

Received 17 April 2013; accepted 5 July 2013

Abstract: The hot tearing susceptibility of $MgZn_{2.5}Y_xZr_{0.5}$ (x=0.5, 1, 2, 4, 6) alloys was evaluated by thermodynamic calculations based on Clyne−Davies model. The microstructure and morphology of hot tearing regions of the alloys were observed by X-ray diffraction and scanning electron microscopy. The solidification temperature and shrinkage stress during the solidification of $MgZn_{2.5}Y_xZr_{0.5}$ alloys in the "T" type hot tearing permanent-mold were acquired with the attached computer. The effect factors of hot tearing susceptibility of $MgZn_{2.5}Y_xZr_{0.5}$ alloys, such as the solidification temperature interval, the variation of solid fraction in vulnerable region, the residual liquid fraction in the final stage, the type of the second phase of the alloys were discussed based on the above calculation and observation. The results demonstrated that the hot tearing susceptibility in the investigated alloys was found as follows: $MgZn_{2.5}Y_2Zr_{0.5}$>$MgZn_{2.5}Y_{0.5}Zr_{0.5}$>$MgZn_{2.5}Y_4Zr_{0.5}$>$MgZn_{2.5}Y_6Zr_{0.5}$>$MgZn_{2.5}Y_1Zr_{0.5}$. The highest hot tearing susceptibility of $MgZn_{2.5}Y_2Zr_{0.5}$ alloy related to the following reasons: the largest freezing range, the biggest changing of the variation of solid fraction in vulnerable region, the least liquid film in the final stage of solidification, the formation of the second phase which worsens the liquid flow and interdendritic feeding after dendrite coherency.

Key words: Mg−Zn−Y−Zr alloys; solidification curve; shrinkage stress; hot tearing susceptibility

1 Introduction

As the lightest commercial engineering structure material, magnesium alloys have attracted great attention because of their low density, high specific strength and stiffness, damping capacity, easy recycling and excellent castability. Up to date, the majority of magnesium products are made by casting. However, magnesium alloys show high susceptibility to hot tearing during the solidification, due to the wide solidification region and high solidification shrinkage stress during casting process [1−4]. For magnesium alloys casting products becoming toward thin wall and complication, hot tearing is to be one of the bottleneck problem of improving the production yield, reducing the cost and enlarging its application [5,6]. In recent years, Mg−Zn−Y−Zr alloy has been developed as a new high strength and deformation magnesium alloy. Zirconium has the same lattice constant as magnesium, so zirconium has been used as heterogeneous nucleation core for magnesium, and it has the great effect of the microstructure refinement [7,8]. Therefore, zirconium has been added into the magnesium alloys as grain refining elements [9]. Yttrium is one of the biggest solid solubility elements in magnesium alloys [10], it has the positive effect on solution strength and aging reinforcement. Yttrium improves the eutectic temperature of magnesium alloy, forms steady second phase at high temperatures. As a result, the precipitation behavior at the grain boundaries is changed for yttrium bared magnesium alloys. This will affect the hot tearing susceptibility of magnesium alloys, which is closely related to grain boundary precipitation behavior [11,12]. The ternary phases formed in the Mg−Zn−Y−Zr alloys are controlled by the contents of Zn and Y and Zn to Y mass ratio [11]. The alloys contain *I*-phase and *W*-phase, *W*-phase, *Z*-phase respectively when Zn to Y ratio is greater than 1, around 1 and less than 1 with the increase of Y content respectively. Intergranular organization form has changed from linear to network one and making the intergranular microstructure coarsen [13]. The different proportions between Zn and Y from 0.42 to 5 are chosen to study the relationship between the different yttrium content and the hot tearing susceptibility through the changes of the second phase and intergranular organization form.

Foundation item: Project (2011BAE22B01) supported by the National Key Technologies R&D Program, China; Project (2013CB632203) supported by the National Basic Research Program of China
Corresponding author: Zheng LIU; Tel: +86-24-25496166; E-mail: zliu4321@vip.sina.com
DOI: 10.1016/S1003-6326(14)63142-3

The aim of the present work is to study the relationship among the hot tearing susceptibility of Mg−Zn−Y−Zr alloys and solidification pathways of magnesium alloys which have the different yttrium content, residual liquid quantity in the final solidification stage and the alteration of the microstructure, and to investigate the temperature and time when hot tearing is generated, and the effects of the solidification fraction and shrinkage stress on hot tearing susceptibility of Mg−Zn−Y−Zr alloys.

2 Experimental

The nominal chemical composition of the Mg−Zn−Y−Zr alloy ingots is shown in Table 1.

Table 1 Chemical composition of tested alloys

Alloy	*w*(Zn)/%	*w*(Y)/%	*w*(Zr)/%	*w*(Mg)/%
Mg−2.5Zn−0.5Y−0.5Zr	2.5	0.5	0.5	Bal.
Mg−2.5Zn−1Y−0.5Zr	2.5	1	0.5	Bal.
Mg−2.5Zn−2Y−0.5Zr	2.5	2	0.5	Bal.
Mg−2.5Zn−4Y−0.5Zr	2.5	4	0.5	Bal.
Mg−2.5Zn−6Y−0.5Zr	2.5	6	0.5	Bal.

SG−5−10 crucible resistance furnace with controllable Si temperature controller was used for melting the alloys. The melting and filling processes were protected under the mixed gas of 0.2% SF_6 and 99.8% nitrogen with the flow rate of 1.6 L/min. Before melting, the inside surface of the stainless steel crucible was sprayed with boron nitride (BN) coatings. The melt was stirred for 5 min then hold at 720 °C for 30 min to ensure the alloying elements dissolved and diffused completely. For the ingot casting, the molten alloy was poured at 720 °C into a "T-shaped" permanent mold preheated to 200 °C. The size and geometry of the "T-shaped" permanent mold are shown in Fig. 1. The "T-shaped" permanent mold was designed to capture the hot tearing in the corner between the spure and the constrained rod. The diameter of the constrained rod near the spure was 12 mm and that in the constrained end was 10 mm. Different diameters in two sides were to lessen the friction between magnesium alloys casting and mold wall in the solidification shrinkage process, so that the measurement results were more accurate. The hot tearing parameters, such as solidification temperature and time, solidification shrinkage stress during magnesium solidification were recorded using analog signal and digital signal conversion [14−16] system, as shown in Fig. 2.

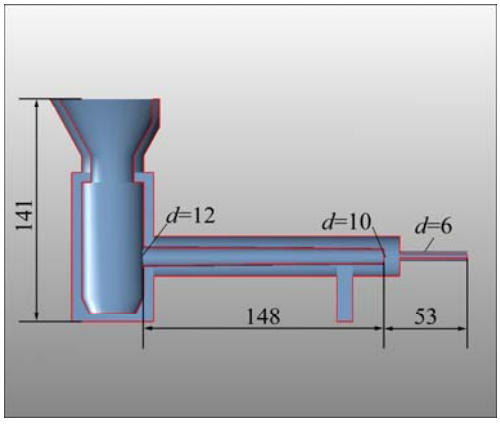

Fig. 1 Schematic of mold for hot tearing (unit: mm)

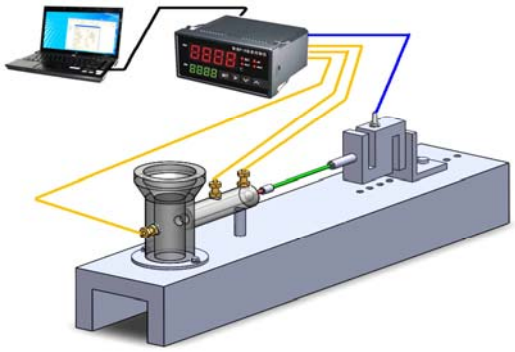

Fig. 2 Schematic of experimental setup

Hot tearing susceptibility of magnesium alloys was evaluated using CSC (cracking susceptibility coefficient) method of Clyne−Davies model [17,18], namely:

$$\mathrm{CSC}=\frac{t_{\mathrm{V}}}{t_{\mathrm{R}}}=\frac{t_{0.01}-t_{0.1}}{t_{0.1}-t_{0.6}}$$

where t_{V} is the time period of the stress release process in vulnerable region; t_{R} is the time period of the stress release process in stress relaxation region.

When the liquid fraction was between 0.1 and 0.6, the interdendritic solidification shrinkage can be feeding at any time because of the sufficient liquid. This stage was known as stress relaxation, so the time of solidification in this stage was defined as t_{R}. With prolonging the solidification time and decreasing the freezing temperature, the liquid fraction was also decreasing, and then the hot tearing susceptibility of the alloys became increasing. The liquid fraction between 0.01 and 0.1 was defined as vulnerable region, and the corresponding solidification time was defined as t_{V}. The ratio of t_{V} and t_{R} is an index to measure the hot tearing susceptibility of alloys. Thus, the effect of alloy composition on the hot tearing was described by using cracking susceptibility coefficient (CSC) in this test. The higher the value of CSC is, the higher the alloy hot tearing susceptibility is. t_{V} and t_{R} can be measured in the curve of liquid fraction and fractional time, as shown in Fig. 3.

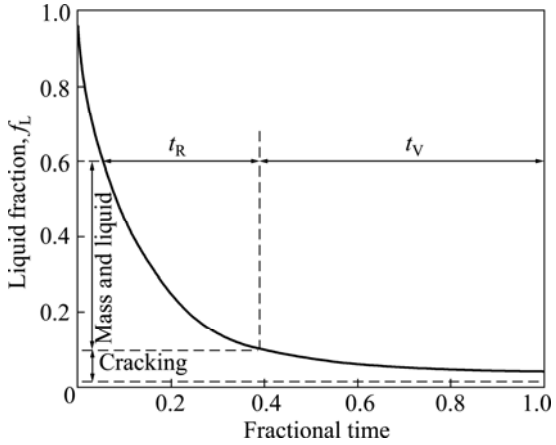

Fig. 3 Method of determination of stress relaxation time t_R and vulnerable time t_V from plot of variation of liquid fraction with fractional time

3 Results and discussion

Figure 4 shows the hot tearing susceptibility of $MgZn_{2.5}Y_xZr_{0.5}$ alloys evaluated with CSC parameters. CSC parameters of $MgZn_{2.5}Y_xZr_{0.5}$ alloys are as follows: CSC ($MgZn_{2.5}Y_2Zr_{0.5}$)>CSC ($MgZn_{2.5}Y_{0.5}Zr_{0.5}$)>CSC ($MgZn_{2.5}Y_4Zr_{0.5}$)>CSC ($MgZn_{2.5}Y_6Zr_{0.5}$)>CSC ($MgZn_{2.5}Y_1Zr_{0.5}$), namely, the highest hot tearing susceptibility is corresponding to $MgZn_{2.5}Y_2Zr_{0.5}$ alloy; the lowest hot tearing susceptibility is corresponding to $MgZn_{2.5}Y_1Zr_{0.5}$ alloy.

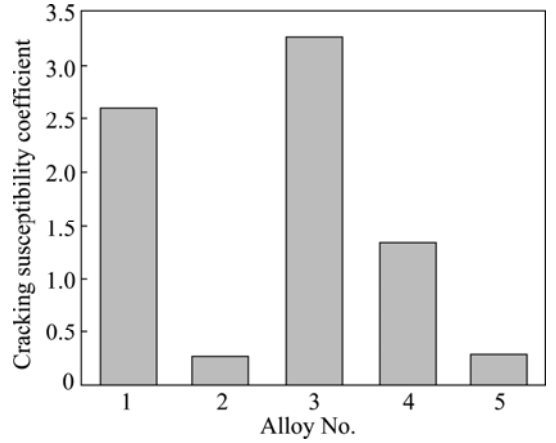

Fig. 4 Hot tearing susceptibility of $MgZn_{2.5}Y_xZr_{0.5}$ alloys: 1—$MgZn_{2.5}Y_{0.5}Zr_{0.5}$; 2—$MgZn_{2.5}Y_1Zr_{0.5}$; 3—$MgZn_{2.5}Y_2Zr_{0.5}$; 4—$MgZn_{2.5}Y_4Zr_{0.5}$; 5—$MgZn_{2.5}Y_6Zr_{0.5}$

Figure 5 shows the relationship between the solidification temperature and the solid fraction. As indicated in Fig. 5, ΔT_C refers to the temperature difference between solid fraction of 0.90 and 0.99. Liquid fraction in this period is much less because of the final stage of solidification. In the ΔT_C period, the formation of dendrite occupies the whole area, and only less amount of residual liquid exists. ΔT_C values of $MgZn_{2.5}Y_1Zr_{0.5}$ and $MgZn_{2.5}Y_6Zr_{0.5}$ alloys are relatively small. The values of ΔT_C for $MgZn_{2.5}Y_1Zr_{0.5}$ and $MgZn_{2.5}Y_6Zr_{0.5}$ alloys are 29.7 °C and 32.2 °C, respectively. ΔT_C for $MgZn_{2.5}Y_2Zr_{0.5}$ alloy is 245.8 °C, which is the highest among the studied alloys. Thus, the shrinkage compensation of $MgZn_{2.5}Y_2Zr_{0.5}$ alloy is the smallest in dendrite separation stage, and the stress which hindered the shrinkage is the largest. In this case, hot tearing is formed easily.

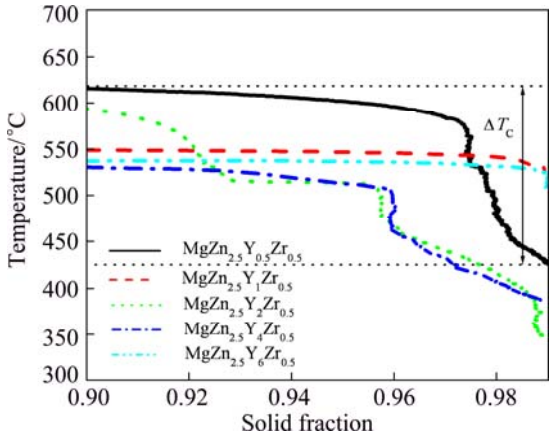

Fig. 5 Relationship between solidification temperature and solid fraction in vulnerable region

Figures 6 and 7 show the solidification curve and solidification temperature range of Mg−Zn−Y−Zr alloys. As can be seen in Fig. 6 that the residual of the liquid fraction of $MgZn_{2.5}Y_2Zr_{0.5}$ alloy in the final stage is the least, but the liquid fractions of $MgZn_{2.5}Y_1Zr_{0.5}$ and $MgZn_{2.5}Y_6Zr_{0.5}$ alloys are the most. From Fig. 7 we can see that the solidification temperature range of $MgZn_{2.5}Y_2Zr_{0.5}$ alloy is the largest, and its value is 299.6 °C. However, solidification temperature ranges of $MgZn_{2.5}Y_1Zr_{0.5}$ and $MgZn_{2.5}Y_6Zr_{0.5}$ alloys are much less, which are 198.7 °C and 177.6 °C, respectively. Generally

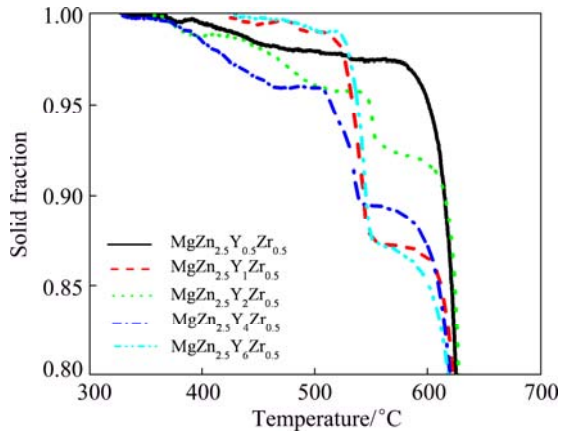

Fig. 6 Curves of solidification of $MgZn_{2.5}Y_xZr_{0.5}$ alloys in final stage

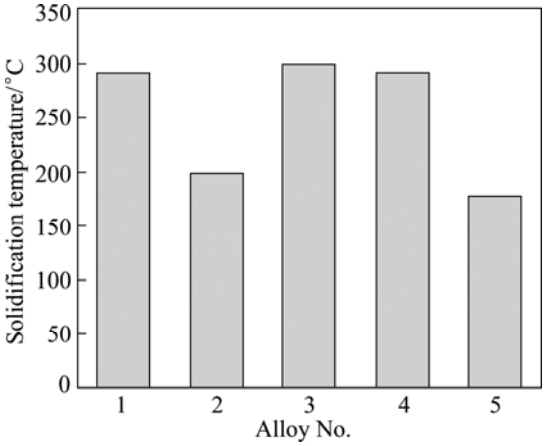

Fig. 7 Solidification temperature of $MgZn_{2.5}Y_xZr_{0.5}$ alloys: 1—$MgZn_{2.5}Y_{0.5}Zr_{0.5}$; 2—$MgZn_{2.5}Y_1Zr_{0.5}$; 3—$MgZn_{2.5}Y_2Zr_{0.5}$; 4—$MgZn_{2.5}Y_4Zr_{0.5}$; 5—$MgZn_{2.5}Y_6Zr_{0.5}$

speaking, the smaller the solidification temperature range, the smaller the hot tearing susceptibility; the higher the residual liquid fraction in the final stage of solidification and the more the liquid film to compensate the solidification contraction. As a result, the hot tearing susceptibility is smaller [19]. So, the hot tearing susceptibility of $MgZn_{2.5}Y_2Zr_{0.5}$ is the highest, $MgZn_{2.5}Y_6Zr_{0.5}$ is the lowest, $MgZn_{2.5}Y_1Zr_{0.5}$, $MgZn_{2.5}Y_{0.5}Zr_{0.5}$ and $MgZn_{2.5}Y_4Zr_{0.5}$ are in the middle.

According to the feeding theory during the solidification process [1], after the dendritic interference point, as the temperature decreases, the feeding mechanism in the solidification process is changed from the overall feeding to the interdendritic feeding gradually. The hot crack caused by shrinkage stress during solidification process is mainly bridged by interdendritic residual liquid in the end of solidification. According to the element repartition theory, Zn and Y will be rejected to the solidification frond end when the primary α-Mg nucleates and grows during the solidification process. With the temperature decreasing, the contents of Zn and Y in intergranular residual liquid are increased, and then the phases rich in Mg, Zn and Y are formed by eutectic reaction before the end of solidification. The ternary phases formed in the Mg−Zn−Y alloys are controlled by the contents of Zn and Y and Zn to Y mass ratio. Figure 8 presents the constituent phases in the as-cast samples identified by X-ray diffraction. As can be seen, with high Zn and low Y contents, the alloys ($MgZn_{2.5}Y_{0.5}Zr_{0.5}$ and $MgZn_{2.5}Y_1Zr_{0.5}$) contain α-Mg, *I*-phase and *W*-phase; with relatively close contents of Zn and Y, the alloy ($MgZn_{2.5}Y_2Zr_{0.5}$) consists of α-Mg and *W*-phase; with low Zn and high Y contents, the alloys ($MgZn_{2.5}Y_4Zr_{0.5}$ and $MgZn_{2.5}Y_6Zr_{0.5}$) consist of α-Mg and *Z*-phase. With high Zn and low Y contents, because α-Mg growth is restrained by the formation of dispersively distributed

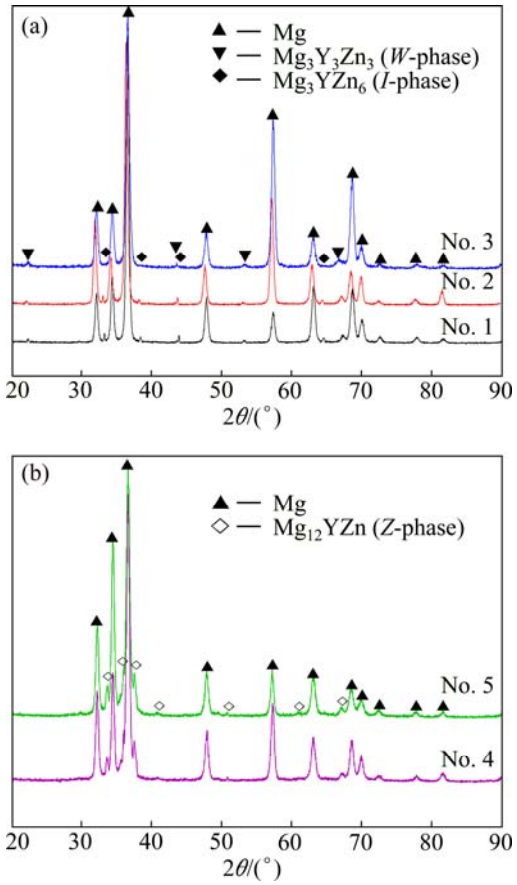

Fig. 8 XRD patterns of $MgZn_{2.5}Y_xZr_{0.5}$ alloys: 1—$MgZn_{2.5}Y_{0.5}Zr_{0.5}$; 2—$MgZn_{2.5}Y_1Zr_{0.5}$; 3—$MgZn_{2.5}Y_2Zr_{0.5}$; 4—$MgZn_{2.5}Y_4Zr_{0.5}$; 5—$MgZn_{2.5}Y_6Zr_{0.5}$

I-phase, α-Mg grains size decreases. Since grains size are smaller, the area and thickness of the liquid film increase due to the increase of the surface area of the grains, and hot tearing susceptibility of the alloy decreases. With proximately Zn and Y contents, the precipitated *W*-phase hinders interdendritic residual liquid flow. It is hard for the interdendrite feeding. This is the main reason for the increased hot tearing susceptibility of $MgZn_{2.5}Y_2Zr_{0.5}$ alloy. With low Zn and high Y contents, the growth of primary α-Mg phase is inhibited by Y-rich region which formed in the front end of the solidification, and consequently interdendritic connection time of the final solidification stage is prolonged. This provides favorable conditions for the feeding channel to keep clear for a longer period of time, and improve the feeding capacity of the alloy between dendritic crystals. But it is easy to make the intergranular microstructure coarsen and connect with each other to form a network at high Y content. The coarsening net-like structure cuts the continuity of the matrix, so it makes the hot tearing susceptibility of the alloy higher. When Y content increases to 6%, the feeding time increases, which means that the residual liquid has enough time to feed the

dendritic separation in the final solidification stage. So the hot tearing susceptibility of the alloy reduces greatly.

Figure 9 shows the contraction force and temperature as a function of time during solidification of $MgZn_{2.5}Y_xZr_{0.5}$ alloys. When Zn content is kept constant, with increase of Y content the situation of hot tearing initiation is different. Figure 9(a) shows the relationship between solidification contraction force and cooling curve of $MgZn_{2.5}Y_{0.5}Zr_{0.5}$ alloy. As can be seen in Fig. 9(a), stress increases sharply at the beginning of the solidification. At the temperature of 475.1 °C and solid phase fraction of 98.0% (as can be seen in Fig. 6), stress has a slight decrease. It is indicated that the hot tearing initiates and propagates at the temperature of 405.5 °C and solid phase fraction of 99.4% (as can be seen in Fig. 6), stress also has a slight decrease, implying that the second hot tearing initiates and propagates. When initial hot tearing generates, the liquid fraction is relatively high, so the hot tearing has been refilled; as the solidification continues, the strength of mushy zone of the alloy is less than solidification shrinkage stress. So the secondary crack generates. Figure 9(b) presents the relationship between solidification shrinkage stress and cooling curve of $MgZn_{2.5}Y_1Zr_{0.5}$ alloy. The figure shows that the shrinkage stress increases with solidification time. At the temperatures of 399.5 °C and 367.7 °C, the solid

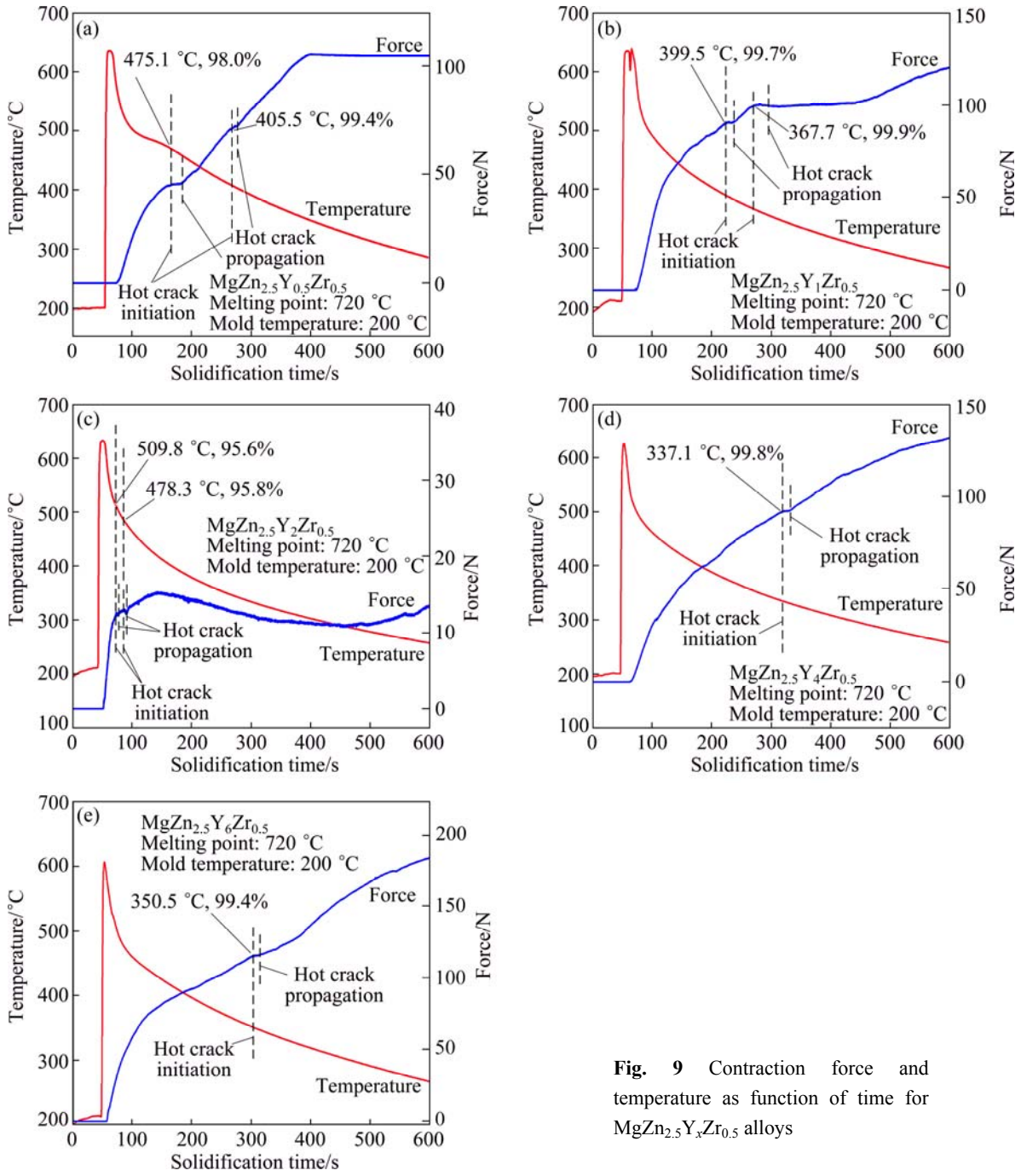

Fig. 9 Contraction force and temperature as function of time for $MgZn_{2.5}Y_xZr_{0.5}$ alloys

fractions of 99.7% and 99.9% (as can be seen in Fig. 6), stress has a slow decrease, having the same meaning with that in Fig. 9(a). In Fig. 9(c), the contraction stress curve of $MgZn_{2.5}Y_2Zr_{0.5}$ alloy decreases sharply at the temperature of 509.8 °C and solid fraction of 95.6% (as can be seen in Fig. 6), and has been in high shrinkage stress position. This is because the second phase precipitation in the solidification process hinders the dendritic feeding, then hot tearing forms when there is enough residual liquid. At the temperature of 478.3 °C and the solid fraction of 95.8% (as can be seen in Fig. 6), the second hot tearing initiates and propagates. Figures 9(d) and 9(e) present contraction force and temperature as a function of time for $MgZn_{2.5}Y_4Zr_{0.5}$ and $MgZn_{2.5}Y_6Zr_{0.5}$ alloys, respectively. At the temperature of 337.1 °C, solid fraction of 99.8% (as can be seen in Fig. 6) and at the temperature of 350.5 °C, solid fraction of 99.4% (as can be seen in Fig. 6), the stress curves become decreasing, but the extend is relatively small. This is not like the other alloys that there are no the second deceasing appearing in the curves, implying the sufficient residual liquid in the final stage of solidification. It is to say that the hot tearing tendencies of the alloys are small.

Because of the solidification shrinkage stress, the already formed hot cracks begin to propagate when dendritic separation has been fed insufficiently by residual liquid. So the information about the initiation and propagation of hot tearing of the alloys is accessible by analyzing the curves of contraction force and temperature as a function of time during solidification. Table 2 shows the information about the initiation and propagation of hot tearing for Mg−Zn−Y−Zr alloys. From Table 2 we can read the hot tearing initiation temperature, the solid fraction, the stress relaxation during the hot tearing propagation, the time of stress relaxation and the rate of stress relaxation. The rate of crack propagation is represented by the rate of solidification shrinkage stress. $MgZn_{2.5}Y_{0.5}Zr_{0.5}$ and $MgZn_{2.5}Y_1Zr_{0.5}$ alloys when the hot tearing is initiated in the alloys have certain strength because the solid fraction is high and the solidification shrinkage stress essentially equals to the interdendritic binding force. So the crack propagation rate is slow. For $MgZn_{2.5}Y_2Zr_{0.5}$ alloy, with the increase of the Y content, the primary precipitated *W*-phase hinders the interdendritic residual liquid flow, making the interdendrite contraction hard to feed. This is the main reason for the formation of initial crack at the lower solid fraction. In the mean time there is sufficient residual liquid to feed, but the strength of mushy zone of alloy is less than the solidification shrinkage stress. As a result, cracks propagate rapidly for the $MgZn_{2.5}Y_2Zr_{0.5}$ alloy. For $MgZn_{2.5}Y_4Zr_{0.5}$ and $MgZn_{2.5}Y_6Zr_{0.5}$ alloys, the growth of primary α-Mg phase is inhibited by Y-rich region which forms in the front end of the solidification, consequently interdendritic connection time of the final solidification stage is prolonged. This is the reason that the feeding capacity of the alloys is improved.

Table 2 Information about initiation and propagation of hot tearing for $MgZn_{2.5}Y_xZr_{0.5}$ alloys

Alloy	Hot crack initiation		Hot crack propagation		
	θ_i/°C	f_{s-i}/%	F_r/N	t_p/s	v_p/(N·s^{-1})
$MgZn_{2.5}Y_{0.5}Zr_{0.5}$	475.1	98.0	0.4762	1.9	0.251
$MgZn_{2.5}Y_1Zr_{0.5}$	399.5	99.7	0.5128	5.9	0.087
$MgZn_{2.5}Y_2Zr_{0.5}$	509.8	95.6	1.2594	1.7	0.741
$MgZn_{2.5}Y_4Zr_{0.5}$	337.1	99.8	0.0977	0.5	0.1954
$MgZn_{2.5}Y_6Zr_{0.5}$	350.5	99.4	0.0367	1.4	0.0262

θ_i is the temperature when cracks generate initially; f_{s-i} is solid fraction when cracks generate initially; F_r is the stress relaxation during crack propagation; t_p is the time of crack propagation; v_p is stress relaxation rate, namely crack propagation rate

Figure 10 shows the surface morphology of the hot tearing of $MgZn_{2.5}Y_xZr_{0.5}$ alloys. As can be seen, the surface of crack covers a layer of film, which is solidified latest and it is the phase with low melting point. Figure 10(a) shows the morphology of crack surface for $MgZn_{2.5}Y_{0.5}Zr_{0.5}$ alloy; the liquid film of crack surface is thin. This is due to the less Y content; the low-melting eutectic phase is unable to form enough liquid film. Irregular columnar dendrite and thinner liquid film are not enough to resist solidification shrinkage stress which stretched dendritic crystal. So the torn liquid film is rarely seen in the picture. Figure 10(b) shows the morphology of crack surface for $MgZn_{2.5}Y_1Zr_{0.5}$ alloy; With Y content increasing, the residual liquid film is thickening. The growth of α-Mg is inhibited by the eutectic phase, so the grain size is obviously smaller than $MgZn_{2.5}Y_1Zr_{0.5}$ alloy. Thus the dendritic crystal ability of resisting the shrinkage stress is improved obviously. As can be seen from Fig. 10(b), the length of the liquid film which has been torn by solidification shrinkage stress increases significantly. Figure 10(c) shows the morphology of crack surface for $MgZn_{2.5}Y_2Zr_{0.5}$ alloy. low-melting point phase can be clearly seen at the grain boundary, and the liquid film has lots of fold, forming the river's pattern. But interdendritic residual liquid flow and interdendritic feeding are hindered by the low- melting point phase. So many micro cracks which have not been filled are left, leading to the higher hot crack tendency of the alloy. Figures 10(d) and (e) present the morphologies of crack surface for $MgZn_{2.5}Y_4Zr_{0.5}$ and $MgZn_{2.5}Y_6Zr_{0.5}$ alloys, respectively. With increasing Y content, the solidification temperature of low-melting point eutectic phase

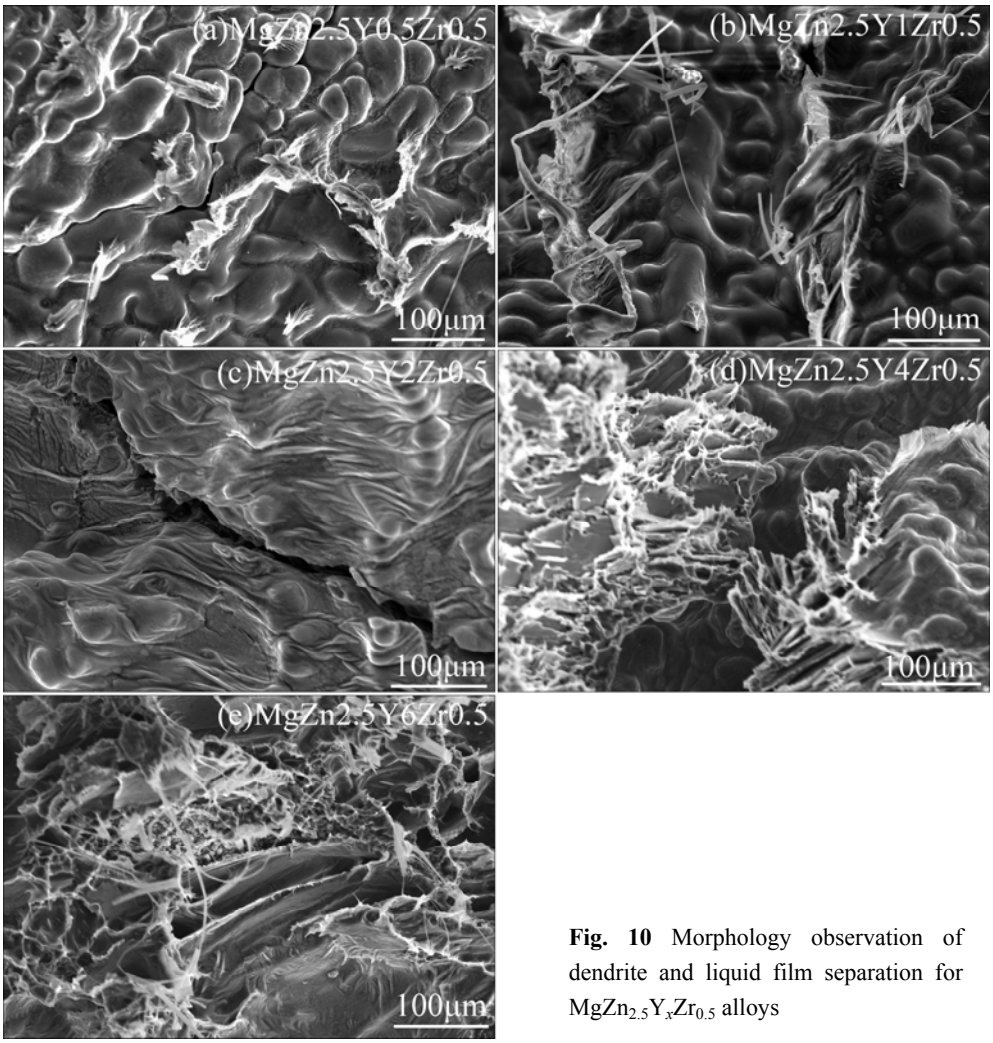

Fig. 10 Morphology observation of dendrite and liquid film separation for $MgZn_{2.5}Y_xZr_{0.5}$ alloys

decreases; liquid film formed in the dendritic grain boundaries becomes thicker, and has more folds. Thus the adhesion of the dendritic grain boundary increases significantly. Liquid film is stretched by the movement of grain, but the tension of liquid film hinders the separation of grain. Columnar crystal is torn and extended significantly, so that it is difficult to form the cracks, which results in the lower tendency of hot crack susceptibility of $MgZn_{2.5}Y_4Zr_{0.5}$ and $MgZn_{2.5}Y_6Zr_{0.5}$ alloys. Generally speaking, the Zn to Y mass ratio plays a key role in the hot tearing susceptibility of $MgZn_{2.5}Y_xZr_{0.5}$ alloys. It is a control factor for the residual liquid, shrinkage stress, separated dendritic crystal in the final stage of solidification and the thickness of liquid film between dendritic grain boundaries.

4 Conclusions

1) The hot tearing susceptibility of $MgZn_{2.5}Y_xZr_{0.5}$ alloys is evaluated by CSC parameters and the relative hot tearing susceptibility of the alloys is as follows: CSC($MgZn_{2.5}Y_2Zr_{0.5}$) > CSC($MgZn_{2.5}Y_{0.5}Zr_{0.5}$) > CSC ($MgZn_{2.5}Y_4Zr_{0.5}$) > CSC($MgZn_{2.5}Y_6Zr_{0.5}$) > CSC ($MgZn_{2.5}Y_1Zr_{0.5}$). Namely, the highest hot tearing susceptibility is according to $MgZn_{2.5}Y_2Zr_{0.5}$ alloy and the lowest one is according to $MgZn_{2.5}Y_1Zr_{0.5}$ alloy.

2) The Zn to Y mass ratio plays an important role in phase composition and microstructure of the alloys, and the ratio is a key factor to control the hot tearing susceptibility. The second phase (*W*-phase) rich in solute is solidified from the interdendritic residual liquid in the final solidification stage and it hinders liquid flowing and prevents the feeding between the dendritic crystals, which makes the hot tearing susceptibility of the alloys higher. But *I*-phase and *Z*-phase mainly inhibit dendritic growth of α-Mg and decrease the grain size, consequently the hot tearing susceptibility of the alloys is reduced.

3) The higher the solidification temperature interval is, the less the residual liquid in the final solidification stage is, and the higher the solidification temperature

change ΔT_C is in the vulnerable region, then the higher the hot tearing susceptibility of the alloys is.

References

[1] DAHLE A K, LEE Y C, NAVE M D, SCHAFFER P L, StJOHN D H. Development of the as-cast microstructure in magnesium−aluminium alloys [J]. Journal of Light Metals, 2001, 1(1): 61−72.

[2] HUANG Yu-guang, WU Guo-hua, WANG Wei, DING Wen-jiang. Research progress and prospects of hot cracking and fluidity of magnesium alloys [J]. Foundry Technology, 2008, 29(3): 416−419. (in Chinese)

[3] QIU Ke-qiang, TAO Si-wei, RE Yan, YOU Jun-hua, REN Ying-lei, LI Rong-de. Effect of Ca on the hot tearing susceptibility of Mg−7Al−2Si casting alloys [J]. Special Casting & Nonferrous Alloys, 2013, 33(2): 91−95. (in Chinese)

[4] QIU Ke-qiang, TAO Si-wei, RE Yan, YOU Jun-hua, REN Ying-lei, LI Rong-de. Effect of strontium addition on the hot tearing susceptibility of Mg−7Al−2Ca−2Si−0.8Zn−0.4Mn casting alloys [J]. Foundry, 2013, 62(2): 19−24. (in Chinese)

[5] HUANG Zhang-hong, ZHANG Yan, CHEN Rong-shi, HAN En-hou. Hot tearing susceptibility of Mg−Zn−Y−Zr alloys [J]. Foundry, 2009, 58(8): 788−792. (in Chinese)

[6] WU Guo-hua, SUN Ming, WANG Wei, DING Wen-jiang. New research development on purification technology of magnesium alloys [J]. The Chinese Journal of Nonferrous Metals, 2010, 20(6) 7−17. (in Chinese)

[7] MA Q, STJOHN D H, FROST M T. Characteristic zirconium-rich coring structures in Mg−Zr alloys [J]. Scripta Materialia, 2002, 46(9): 649−654.

[8] QIAN M, GRAHAM D, ZHENG L. A new zirconium-rich master alloy for the grain refinement of magnesium alloys [J]. Mater Sci Technol, 2003, 19: 156−162.

[9] HUANG Zhang-hong, QU Heng-lei, FU Zhao-di, SUN Dan, SHU Ying, YANG Jian, YANG Jian-chao. Effect of Zr on microstructure and solidification behavior of Mg−Zn−Y alloys [J]. Heat Treatment of Metals, 2011, 36(9): 10−12. (in Chinese)

[10] YU Jue-qi, YI Wen-zhi. Binary alloy phase-diagrams [M]. Shanghai: Shanghai Science and Technology Press, 1987. (in Chinese)

[11] YANG Shu-qi, GUO Hua-ming, LIU Zi-li. Effects of Y on microstructure and mechanical properties of Mg−Zn alloys [J]. Materials for Mechanical Engineering, 2007, 31(8): 60−63. (in Chinese)

[12] LI Min, WANG Hong-wei, ZHU Zhao-jun, WEI Zun-jie. Effects of scraps and yttrium on the as-casting microstructure, hot tearing and solidification characteristics of ZL205A alloy [J]. Rare Metal Materials and Engineering, 2010, 39(s1): 10−15. (in Chinese)

[13] LEE J Y, KIM D H Y, KIM H Y K, KIM D H. Effects of Zn/Y ratio on microstructure and mechanical properties of Mg−Zn−Y alloys [J]. Materials Letters, 2005, 59(29−30): 3801−3805.

[14] ZHEN Z, HORT N, HUANG Y. Quantitative determination on hot tearing in Mg−Al binary alloys [J]. Materials Science Forum, 2009, 618−619: 533−540.

[15] ZHEN Z, HORT N, UTKE O. Investigations on hot tearing of Mg−Al binary alloys by using a new quantitative method [C]// NYBERG E A, AGNEW S R, NEELAMEGGHAM N R, PEKGULERYUZ M O. Magnesium Technology 2009. America: The Minerals, Metals and Materials Society, 2009: 105−110.

[16] ZHEN Z, UTKE O, PUNESSEN W. Apparatus for determining the hot tearing susceptibility of metallic melts: America US, 201010000702Al [P]. 2010−01−07.

[17] CLYNE T W, DAVIES G J. The influence of composition on solidification cracking susceptibility in binary alloy systems [J]. Brit Found, 1981, 74: 65−73.

[18] CLYNE T W, DAVIES G J. A quantitative solidification cracking test for castings and an evaluation of cracking in Al−Mg alloys [J]. Brit Found, 1975, 68: 238−244.

[19] PUMPHREY W I, JENNINGS P H. A consideration of the nature of brittleness above the solidus in castings and welds on aluminum alloys [J]. J Inst Met, 1948, 75: 235−256.

稀土钇对 Mg−Zn−Y−Zr 合金热裂敏感性的影响

刘 正，张斯博，毛萍莉，王 峰

沈阳工业大学 材料科学与工程学院，沈阳 110870

摘 要：通过 Clyne−Davies 模型对 $MgZn_{2.5}Y_xZr_{0.5}$(x=0.5, 1, 2, 4, 6)系合金的热裂敏感性进行预测；采用 X 射线衍射和扫描电子显微镜分别对 $MgZn_{2.5}Y_xZr_{0.5}$ 系合金进行显微组织和热裂区域组织形貌观察，并用自制的“T”形热裂模具，通过 A/D 转换，用计算机对 $MgZn_{2.5}Y_xZr_{0.5}$ 系合金凝固过程中的温度、收缩应力信号数据进行采集和进一步的处理，并描绘其曲线。研究 $MgZn_{2.5}Y_xZr_{0.5}$ 合金的凝固温度区间、脆弱区域的凝固温度变化、凝固最后阶段剩余液相分数以及合金中第二相种类等因素对 $MgZn_{2.5}Y_xZr_{0.5}$ 系合金热裂倾向的影响：合金热裂倾向从大到小顺序为 $MgZn_{2.5}Y_2Zr_{0.5}$，$MgZn_{2.5}Y_{0.5}Zr_{0.5}$，$MgZn_{2.5}Y_4Zr_{0.5}$，$MgZn_{2.5}Y_6Zr_{0.5}$，$MgZn_{2.5}Y_1Zr_{0.5}$。由于 $MgZn_{2.5}Y_2Zr_{0.5}$ 合金的凝固温度区间最宽，脆弱区域的凝固温度变化最大，凝固最后阶段形成的液膜最少，枝晶干涉点后析出的第二相阻碍枝晶间的补缩等多种原因而造成合金的热裂倾向最大。

关键词：Mg−Zn−Y−Zr 合金；凝固曲线；收缩应力；热裂敏感性

(Edited by Hua YANG)